Localization of Subthalamic Nucleus Borders Using *Macroelectrode* Local Field Potential Recordings

I.Telkes[1], N.F.Ince[1], I. Onaran[1], A. Abosch[2]

Abstract— **Deep brain stimulation of the subthalamic nucleus (STN) is a highly effective treatment for motor symptoms of Parkinson's disease. However, precise intraoperative localization of STN remains a procedural challenge. In the present study, local field potentials (LFPs) were recorded from DBS macroelectrodes during trajectory to STN, in six patients. The frequency-vs-depth map of LFP activity was extracted and further analyzed within different sub-bands, to investigate whether LFP activity can be used for STN border identification. STN borders identified by LFPs were compared to border predictions by the neurosurgeon, based on microelectrode-derived, single-unit recordings (MER-SUA). The results demonstrate difference between MER-SUA and macroelectrode LFP recording with respect to the dorsal STN border of -1.00 ±0.84 mm and -0.42 ±1.07 mm in the beta and gamma frequency bands, respectively. For these sub-bands, RMS of these distances was found to be 1.26 mm and 1.06 mm, respectively. Analysis of other sub-bands did not allow for distinguishing the caudal border of STN. In conclusion, macroelectrode-derived LFP recordings may provide an alternative approach to MER-SUA, for localizing the target STN borders during DBS surgery.**

I. Introduction

Deep brain stimulation (DBS) of the subthalamic nucleus (STN) is an effective therapy for the treatment of the motor symptoms of Parkinson's Disease (PD) [1]. DBS involves the surgical implantation of a quadripolar electrode into the motor territory of STN, followed by chronic stimulation via connection of the electrode to an implanted pulse generator (IPG). An important factor contributing to the efficacy of DBS is the accurate localization of STN in the brain. The small volume of STN motor territory, its depth from the cortical surface, and its proximity to other critical neural structures, make precise targeting crucial as well as challenging [2]. Together with stereotactic imaging, intra-operative microelectrode recording (MER) is the most commonly used physiological technique to determine STN location for chronic implantation of DBS macroelectrode [3]. In MER, single-unit activity (SUA), i.e., the electrical activity resulting from individual neurons, is recorded by microelectrodes characterized by small diameter and high impedance. The resulting signal patterns are interpreted in order to localize the anatomical borders of STN [4]. The initial trajectory and stereotactic coordinates of the target are determined based on preoperative MRI and/or CT images. Microelectrodes are then inserted through cannulas into the brain and SUAs are recorded [5]. The number of MER trajectories being used in localization can vary based on technical factors and institutional preference from one to five or more [1]. Following MER target localization, microelectrodes are withdrawn and replaced by the quadripolar DBS macroelectrode. Although MER provides useful information for guiding surgery, the procedure carries a risk of intracranial hemorrhage due to usage of multiple electrodes and sharp tip of these microelectrodes [6]. Moreover, the interpretation of signal characteristics by neurophysiologists or neurosurgeons makes the procedure more open to human error with the increased surgical time, especially in the multi-target cases requiring MER interpretation that is more complex [4].

Unlike MER-SUA, macro electrode recordings are based on local field potentials which represent the aggregate activity of neuronal populations in the region of the electrode contact [7]. In PD, LFP recordings from STN are an important indicator of neural rhythms [8]. Studies have demonstrated an excessive synchrony in beta band (13-30 Hz) activity in STN [9].

The aim of the present study was to explore the informational content of LFPs recorded from macro DBS electrodes, in order to identify the anatomical borders of STN. Since LFPs can easily be recorded from macro contacts, their use in the operating room can reduce surgery time and serve as a useful tool for target validation.

II. Methods

A. Patients and surgery

Six patients provided informed consent and with approval of the University of Minnesota Institutional Review Board were enrolled in this study. All study subjects had a diagnosis of idiopathic PD and exhibited typical

Research supported by National Science Foundation, award CBET-1067488.

1.N.F.I. is with the Biomedical Engineering Department, University of Houston, Texas, 77204-5060, USA, (corresponding author: (713) 743 4461; e-mail: nfince@uh.edu). Senior IEEE Member

1.I.T. is with the Biomedical Engineering Department, University of Houston, Texas, 77204-5060, USA, (e-mail: itelkes@uh.edu).

1. I.O. is with the Biomedical Engineering Department, University of Houston, Texas, 77204-5060, USA, (e-mail: onaran@gmail.com).

2.A.A. is with the Department of Neurosurgery, Director of Stereotactic and Epilepsy Surgery, Director of Neurosurgery Research, University of Colorado, Aurora, CO 80045, USA (e-mail: aviva.abosch@ucdenver.edu)

Parkinsonian motor symptoms despite optimal medial therapy. All patients discontinued Parkinson's medications 12 hours prior to surgery. Per standard clinical routine in our institution, three simultaneous MER-SUA recording tracks were performed in each subject using local anesthetic alone. The initial target and trajectory were identified by stereotactic MRI fused to a stereotactic CT on a neuronavigational platform (StealthStation, Medtronic Corp, CO). Microelectrode implantation and simultaneous SUA recordings were obtained using a Neurodrive and Microguide system (AlphaOmega Inc., USA) respectively. Following MER-SUA, all patients underwent unilateral implantation of a DBS electrode into STN (DBS electrode model # 3389: Medtronic Corp, Fridley, MN). These DBS electrodes contain four platinum–iridium cylindrical surfaces from deepest contact 0 to most superficial contact 3 (1.27 mm diameter and 1.5 mm length) and a center-to-center distance of 2 mm.

B. Recordings

STN LFPs were recorded with XLTEK-EMU128FS system (Natus, San Carlos, California). The initial monopolar LFP recording generally started 20 mm above the estimated target and continued until the electrode reached -3 mm below MER-determined target. The Neurodrive was used to drive the electrode down to the estimated target using 1 mm steps until 10 mm above estimated target and then the step size was reduced to 0.5 mm. LFP data were recorded from all four contacts of the DBS electrode along with EKG signal for 30 seconds at each depth. Signals were sampled at 2 kHz with 16 bit A/D resolution. All raw data channels were high-pass filtered at 0.1 Hz. Signals were transferred into a PC for off-line spectral analysis.

C. Analysis

Recorded LFP data were annotated and visualized in the XLTEK system and then exported into MATLAB (Mathworks, Natick, Massachusetts) for processing. LFP data from all four contacts were low-pass filtered using an FIR filter with a 450-Hz cutoff frequency, and then down-sampled to 1000 Hz for analysis [8]. During preprocessing of LFP data, monopolar signals were converted into bipolar derivation (0-1, 1-2, 2-3). It should be noted that each bipolar contact represents the LFP activity at different depths with 2 mm spacing. Consequently, LFP data derived from all bipolar contacts (which sample different depths) were combined and processed together.

In order to explore the frequency content of the LFP data at each depth, we generated a depth-frequency analysis similar to a time-frequency analysis. We observed that the LFP data were corrupted by many factors including tremor and/or environmental factors in the operating room setting. Therefore, we computed the LFP spectrum with a modified Welch periodogram method, including robust statistics. Simply, rather than using an average over different segments, we used a median operator to compute the periodogram which suppressed outliers. Specifically, for spectrum analysis, the fast Fourier transform (FFT) was computed with a 512 samples long Hanning window and the window was shifted with 50% overlap. After computing the squared magnitude in each sliding window, we used the median operator to estimate the LFP spectrum. We repeated this same procedure at each depth and the resulting spectra were used to visualize dynamic frequency spectrum of the LFP data.

C. Post-Processing

We investigated the depth-frequency maps and extracted the energy of LFP sub-bands at each depth to identify the superior STN border. The sub-band energy values at each depth were first filtered by zero-phase filtering in both forward and reverse directions to smooth the data. Then, output was interpolated with 0.5 mm resolution. Instead of joining data points by straight line segments using a linear interpolation, a cubic interpolation method was chosen. Finally, the interpolated signal was normalized between zero and one with a Max-Min method.

In order to identify the superior STN border using normalized sub-band energy features, we first determined a 10% threshold to find noticeable energy increase with respect to higher depth values. Then, we computed the first derivative of the data to inspect the change in energy of consecutive data points. We identified the superior STN border using the following criteria:

- energy value exceeds the 10% threshold
- the slope of the signal is positive for the three consecutive points
- the slope was taken into account after 7 mm and below

In order to compare the borders identified by MER-SUA and LFP, a paired student t-test was conducted. Moreover, the root mean square (RMS) of these differences was calculated.

I. RESULTS

The raw LFP data of a representative subject is shown in Fig. 1A. Typical artifacts which resulted from abrupt movements of the patient and other environmental factors can be seen at the higher depths. After the electrode reached a certain depth, high amplitude LFP activity was observed. This amplitude change occurred consistently in all subjects between the superior and inferior border of STN as identified by MER-SUA. To give a flavor about the frequency content of LFP activity at various depths, the depth-frequency map of the same subject is shown in Fig. 1B. We observed a clear increase in beta-band energy within the STN borders (as defined by MER-SUA).

Surprisingly, excessive LFP activity was not limited to the beta-band but was also observed at higher bands, ranging up to 450Hz. Based on these observations, we decided to use beta (13-30Hz) and gamma frequency bands (48-450Hz) for localization of STN border. Similarly, filtered LFP signals

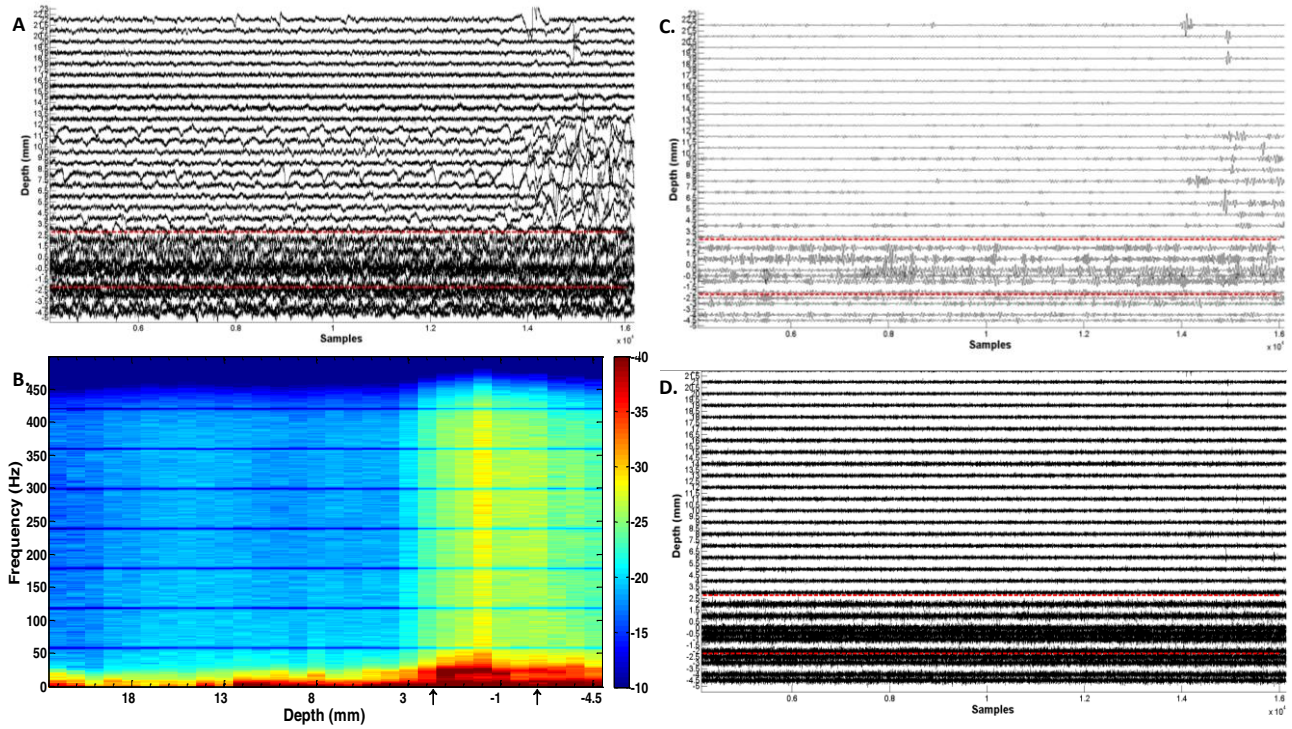

Fig.1. (A) The raw LFP data of a representative subject while the electrode moved from 22 mm above the target down to -4.5 mm below it. (B) Spectral Analysis for the representative subject. High pass filtered at 2.5 Hz. Black arrows show the superior and inferior STN borders, respectively from left to right. (C) Bipolar LFPs band passed filtered at 13-30 Hz for the representative subject. (D) Bipolar LFPs high pass filtered at 48 Hz. Red dashed lines show the upper and bottom borders of STN, respectively.

indicate an increasing trend inside the STN in these bands (Fig.1C-D) that may provide an alternative approach to localize the borders.

In Fig.2, the sub-band energy plots for all subjects in the beta and gamma bands are demonstrated. The sub-band data of all subjects were normalized to its maximum value and aligned with respect to the average superior border of the STN (red dashed line). Except one subject, (data in orange color) in all cases the beta band energy is well correlated with the STN superior border.

Figure 3 shows the variance values of representative subject with the differences of consecutive data points at each depth at beta band. In order to select the superior border of STN, a 10% threshold was applied and the first data point below 7 mm passing the threshold and having a positive slope (increasing energy trend) was selected as the superior border. Up to 7 mm, all subjects were having a consistent variance and 7 mm was the first point having an increased standard deviation (pink shaded area) from the average and the unlikely possibility of above depths being top border (10 mm is corresponding 7 mm above the average superior border), 7 mm was chosen as threshold depth value.

The mean value of superior STN border estimated with MERs was 3.61 ±0.92 mm while the mean value of superior border derived from macro electrode LFP recordings was 4.67 ±1.03 mm and 4.08 ±1.56 mm in beta and gamma bands, respectively. The root mean square (RMS) of the

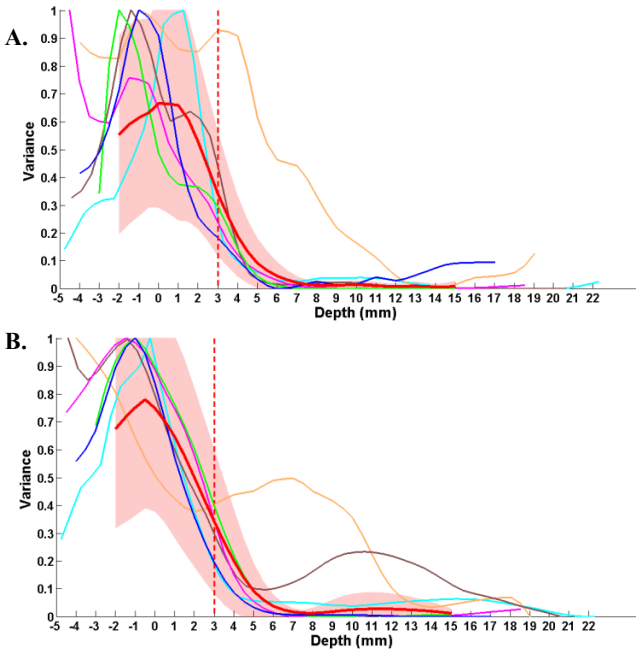

Fig.2. Variance-vs-depth plot for all patients. (A) Band pass filtered at 13-30 Hz. (B) High pass filtered at 48 Hz. The red line shows the mean variance value along the depths and the pink shaded area shows the ±standard deviation around the mean. Data in orange is excluded.

difference between MER and LFP was 1.26 mm in beta and 1.06 mm at gamma band. The mean ± standard deviation of distance was -1.00 ±0.84 mm and -0.42 ±1.07 mm in beta

and gamma bands, respectively. Student t-test analysis pointed that the differences between macroelectrode recordings and MERs were statistically significant for beta band ($p=0.03<0.05$), however non-significant for gamma band ($p=0.38>0.05$).

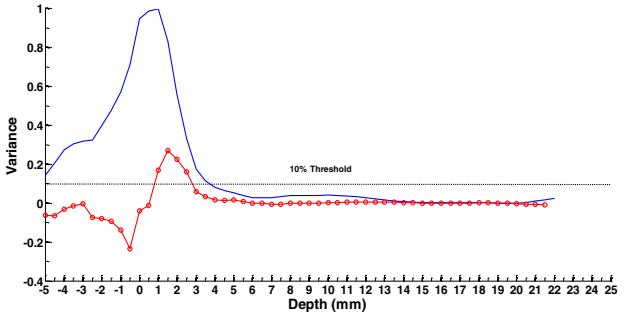

Fig.3. Variance vs depth plot with the differences between each consecutive data points for a representative patient. Band pass filtered at 13-30 Hz. Blue curves shows the variance. Red curve shows the difference of consecutive points along the data. Black line is the 10% threshold.

II. DISCUSSION

Previous studies suggested that the excessive beta-band activity of LFP can be used to localize STN [7]. In the present study, during a DBS electrode implantation surgery, we recorded LFPs from four contacts of DBS macro electrodes in six patients. We observed increased LFP activity between the superior and inferior STN borders. After computing the LFP spectrum at each depth, we observed that excessive activity occurs not only in the beta-band, but also in the higher bands, ranging from 40 up to 450 Hz. Subsequent data analysis has shown that the localization error of superior STN border between macro electrode recordings and MER SUA was around 1 mm in both beta and gamma band. These results support the use of intraoperative macro-electrode recordings, in conjunction with preoperative stereotactic imaging for target localization in PD. Due to the more robust nature of the LFP signal-derived from populations of neurons, instead of single neurons, LFP signal based confirmation of DBS location might be more advantageous than MER-SUA. LFP-based DBS surgery might also lend itself to a more automated approach to interpreting complex intraoperative neurophysiology rather than the current scenario that requires significant expertise in auditory MER-SUA interpretation. It should be also noted that due its comparatively large contact size and between contact spacing, the DBS macro electrode has poor spatial resolution than the MER. For instance, for a bipolar contact derivation, at least a 3.5 mm displacement is required for both contacts to pass through a structure. In contrast, MER is characterized by superior spatial resolution as the SUA activity is recorded from the tip of the microelectrode, which has a length of several microns in length. Another drawback of the study is regarding only the superior border of the STN. In DBS surgery, the target depth is primarily the inferior border of STN rather than the superior border. However, because of the risk of serious side effects in case of further insertion of electrode, it is difficult to record data from lower depths.

ACKNOWLEDGMENT

This research was supported by National Science Foundation, award CBET-1067488.

REFERENCES

[1] H. Cagnan, K. Dolan, X. He, M. F. Contarino, R. Schuurman, P. van den Munckhof, W. J. Wadman, L. Bour, and H. C. F. Martens, "Automatic subthalamic nucleus detection from microelectrode recordings based on noise level and neuronal activity.," *J. Neural Eng.*, vol. 8, no. 4, p. 046006, Aug. 2011.

[2] P. Krack, M. I. Hariz, C. Baunez, J. Guridi, and J. A. Obeso, "Deep brain stimulation : from neurology to psychiatry ?," *Trends Neurosci.*, vol. 33, no. 10, pp. 474–484, 2010.

[3] A. Zaidel, A. Spivak, L. Shpigelman, H. Bergman, and Z. Israel, "Delimiting subterritories of the human subthalamic nucleus by means of microelectrode recordings and a Hidden Markov Model.," *Mov. Disord.*, vol. 24, no. 12, pp. 1785–93, Sep. 2009.

[4] T. A., "An automated navigation system for deep brain stimulator placement using hidden Markov models," *Neurosurgery.*, vol. 10.1227/01, pp. 108–17, 2010.

[5] K. P. Michmizos, G. L. Tagaris, D. E. Sakas, K. S. Nikita, and S. Member, "Automatic Intra-Operative Localization of STN using the Beta Band Frequencies of Microelectrode Recordings," pp. 1–6.

[6] H. Xiaowu, J. Xiufeng, Z. Xiaoping, H. Bin, W. Laixing, C. Yiqun, L. Jinchuan, J. Aiguo, and L. Jianmin, "Risks of intracranial hemorrhage in patients with Parkinson's disease receiving deep brain stimulation and ablation.," *Parkinsonism Relat. Disord.*, vol. 16, no. 2, pp. 96–100, Feb. 2010.

[7] C. C. Chen, A. Pogosyan, L. U. Zrinzo, S. Tisch, P. Limousin, K. Ashkan, T. Yousry, M. I. Hariz, and P. Brown, "Intra-operative recordings of local field potentials can help localize the subthalamic nucleus in Parkinson's disease surgery.," *Exp. Neurol.*, vol. 198, no. 1, pp. 214–21, Mar. 2006.

[8] N. F. Ince, A. Gupte, T. Wichmann, J. Ashe, T. Henry, M. Bebler, L. Eberly, and A. Abosch, "Selection of optimal programming contacts based on local field potential recordings from subthalamic nucleus in patients with Parkinson's disease.," *Neurosurgery*, vol. 67, no. 2, pp. 390–7, Aug. 2010.

[9] N. Jenkinson and P. Brown, "New insights into the relationship between dopamine, beta oscillations and motor function.," *Trends Neurosci.*, vol. 34, no. 12, pp. 611–8, Dec. 2011.